Biochemistry

 Volume 33, Number 18 May 10, 1994

Accelerated Publications

^{1}H NMR Studies of the High-Affinity Rev Binding Site of the Rev Responsive Element of HIV-1 mRNA: Base Pairing in the Core Binding Element†

Robert D. Peterson,‡ David P. Bartel,§ Jack W. Szostak,§ Suzanna J. Horvath,‖ and Juli Feigon*,‡

Department of Chemistry and Biochemistry and Molecular Biology Institute, University of California, Los Angeles, California 90024, Department of Molecular Biology, Massachusetts General Hospital, Boston, Massachusetts 02114, and Division of Biology, 147-75, California Institute of Technology, Pasadena, California 91125

Received October 15, 1993; Revised Manuscript Received March 11, 1994®

ABSTRACT: ^{1}H NMR studies of a 30-nucleotide RNA oligonucleotide (RBE3), which contains a high-affinity binding site for Rev of the HIV-1 Rev responsive element (RRE), two derivatives of RBE3 (RBE3AA and RBE3-A), and the complex of RBE3 with peptides derived from the RNA binding domain of HIV-1 Rev, are presented. The high-affinity binding site of the RRE consists of an asymmetric internal loop and surrounding Watson–Crick base pairs. In the wild-type RRE, one of the stems is closed by a loop; this is replaced in REB3 by the stable UUCG tetraloop. NOE data suggest that the internal loop of the free RNA contains structural features that have been predicted on the basis of *in vitro* selection experiments [Bartel, D. P., *et al.* (1991) *Cell 67*, 529–536]. The structural features include a G_{syn}·G_{anti} base pair, a G_{anti}·A_{anti} base pair, and a looped out U. When the Rev peptide is bound to the RNA, the base pairs in the internal loop appear to be stabilized, although the RNA chemical shifts indicate that the RNA conformation undergoes some changes when bound by Rev peptide.

The genome of HIV type 1 (HIV-1) codes for two essential regulatory proteins, Tat and Rev (Rosen, 1991; Steffy & Wong-Staal, 1991). Rev carries out its regulatory function by binding to a specific mRNA sequence from HIV-1, called the Rev responsive element (RRE) (Rosen *et al.*, 1988; Daly *et al.*, 1989; Felber *et al.*, 1989; Malim *et al.*, 1989; Zapp & Green, 1989; Cochrane *et al.*, 1990). This interaction between Rev and the RRE mediates the transition from early to late gene expression by enhancing the expression of the structural proteins, which are translated from singly spliced and unspliced HIV-1 mRNA. The interaction of Rev with the RRE has been proposed to be important in facilitating the nuclear export of the incompletely spliced mRNAs (Malim *et al.*, 1989; Emerman *et al.*, 1989; Felber *et al.*, 1989; Hammarskjöld *et al.*, 1989), in regulation of splicing of HIV mRNA (Chang & Sharp, 1989; Lu *et al.*, 1990; Kjems *et al.*, 1991b; Kjems & Sharp, 1993), and in increasing the translation efficiency of the structural proteins from these mRNAs (Lawrence *et al.*, 1991; D'Agostino *et al.*, 1992).

The RRE has been mapped to a 234-nucleotide fragment of the HIV-1 genome, which is located within the envelope gene (Rosen *et al.*, 1988; Felber *et al.*, 1989; Malim *et al.*, 1989). Mutational analysis and RNase protection experiments have shown that a 66-nucleotide fragment, domain II of the RRE, is sufficient for high-affinity binding of Rev *in vitro* (Malim *et al.*, 1990; Heaphy *et al.*, 1990; Holland *et al.*, 1990) and that domain II alone is sufficient for a detectable

† This work was supported by NIH Grant P01 GM 39558 and NSF Presidential Young Investigator Award DMB 89-58280 with matching funds from AmGen Inc., DuPont/Merck Pharmaceuticals, Monsanto Co., and Sterling Drug Inc. (J.F.), by NIH Predoctoral Training Grant GM 07185 (R.D.P.), and by Hoechst AG (D.P.B. and J.W.S.).

* Corresponding author.
‡ University of California, Los Angeles.
§ Massachusetts General Hospital.
‖ California Institute of Technology.

® Abstract published in *Advance ACS Abstracts*, April 15, 1994.

0006-2960/94/0433-5357$04.50/0

Rev responsiveness *in vivo* (Huang *et al.*, 1991). Rev binds first to a high-affinity binding site in the RRE and that subsequently additional Rev molecules oligomerize along adjacent lower affinity binding sites on the RRE (Heaphy *et al.*, 1990, 1991; Malim & Cullen, 1991; Kjems *et al.*, 1991a). It is thought that this complex between the RRE and multiple copies of Rev then carries out the regulatory functions. The high-affinity binding site of Rev on the RRE has been more precisely localized to nucleotides 45–75 of the RRE by iterative *in vitro* selection (Bartel *et al.*, 1991; Tuerk *et al.*, 1993), mutational analysis (Cook *et al.*, 1991; Heaphy *et al.*, 1991; Dayton *et al.*, 1992), chemical protection and modification (Kjems *et al.*, 1992; Tiley *et al.*, 1992), and nucleotide analogue (Iwai *et al.*, 1992) studies.

Bartel *et al.* (1991) concluded that the essential bases of Rev binding were 45–53 and 65–75 (core binding element) which form base-paired stems on either side of an asymmetric internal loop which contains interspersed Watson–Crick and noncanonical base pairs. The bases outside this region are important for stabilizing these stems, but their sequence, including the hairpin loop, is relatively unimportant. Within the internal loop, a G48·G71 *syn·anti* base pair was proposed on the basis of covariation of these bases to A48 and A71, which can form an isosteric base pair. A possible pairing between G47 and A73 was also suggested. Additional evidence for these noncanonical base pairs has recently been found by Iwai and co-workers, who performed binding studies with Rev and a series of synthetic RRE RNAs containing chemical modifications at several sites (Iwai *et al.*, 1992).

A 17 amino acid peptide containing the RNA binding domain of Rev, Rev17 (Figure 1E) (Kjems *et al.*, 1991b), has been shown to bind to a short segment of the RRE, containing the high-affinity binding site, with a K_d of 0.2 nM (Tan *et al.*, 1993). A variant of this peptide, Rev22 (Figure 1F), binds this RNA with a K_d of 0.013 nM (Tan *et al.*, 1993). These functional Rev peptides together with the minimal RNA Rev binding elements provide a convenient model system for studying the interaction of Rev with the RRE.

We have studied the solution conformation of RBE3 (Figure 1B) (Bartel *et al.*, 1991), a 30-nucleotide RNA which contains the core binding element of the RRE, and two mutants of this sequence, RBE3-A and RBE3AA (Figure 1C,D). In RBE3, three base pairs and the hairpin loop of stem–loop IIB of the RRE are replaced with the stable hairpin loop C(UUCG)G. Our results suggest that the internal loop of the free RBE3 is conformationally flexible but has a predominant conformation which contains the proposed G48·G71 and G47·A73 base pairs as well as a looped out U. We have also studied the conformation of RBE3 bound by each of the two peptides, Rev17 and Rev22. The Rev peptides bind specifically but not as tightly as expected to RBE3, and some RNA structural changes occur on Rev peptide binding. However, the major structural features seen in the internal loop of the free RNA are still present in the bound form.

MATERIALS AND METHODS

Sample Preparation. RNA oligonucleotides RBE3 (GGUGGGCGCAGCUUCGGCUGACGGUACACC), RBE3-A (GGUGGGCGCAGCUUCGGCUGCGGUACACC), and REB3AA (GGUGGACGCAGCUUCGGCUGACGAUACACC) were prepared by *in vitro* transcription using T7 RNA polymerase and the DNA oligonucleotides d(GCGTAATACGACTCACTATAG) (T7 promoter) and d(GGTGTACCGTCAGCCGAAGCTGCGCCCACCTATAGTGAGTCGTATTACGC) (template strand), by modification of the procedures described by Milligan *et al.* (1987) and Wyatt *et al.* (1991). Transcription reaction volumes were 75 mL and typically yielded 10 mg of RNA of the desired sequence. NTPs were obtained from Pharmacia. The T7 RNA polymerase was purified from the overproducing strain *E. coli* UT4400/pGP1-5/pGP1-1 (gift from Dr. Stanley Tabor) by modification of the procedure of Zawadzki and Gross (1991). After transcription, the RNA was phenol extracted and purified by preparative scale electrophoresis on denaturing polyacrylamide gels. Typically, one 75-mL transcription required 10 gels (42 cm × 33 cm × 1 cm). The correct RNA band was identified by UV shadowing, cut out, extracted from the gel by electroelution, and concentrated by ethanol precipitation. NMR samples were prepared by dissolving the RNA in 10 mM sodium phosphate, pH 6.0, 1 M NaCl, and 10 mM EDTA and dialyzing in Amicon Centricon 3 filter units and then repeating the dialysis with NMR buffer (usually 10 mM sodium phosphate, pH 6, and 100 mM NaCl).

The peptides Rev17 and Rev22 (Tan *et al.*, 1993) were synthesized on an ABI 430A peptide synthesizer using *t*-Boc chemistry. Succinylation of the N terminus of Rev22 was carried out by 20-min reaction with 0.5 M succinic anhydride. After removal of the side-chain protecting groups and cleavage of the peptide off the resin using anhydrous liquid HF in the presence of *p*-cresol and *p*-thiocresol as scavengers (60 min at 0 °C), the peptide was desalted on AG1-X2 Dowex resin. Residual scavengers were removed by chromatography on Sephadex G-25. Peptides were stored lyophilized until used. Sequence and purity of the peptides were confirmed by analytical reverse-phase HPLC, amino acid analysis, sequence analysis, and mass spectrometry.

NMR Spectroscopy. NMR spectroscopy was done at 500 MHz on a GE GN500 NMR spectrometer. One-dimensional spectra in H_2O were collected over a range of temperatures from 1 to 50 °C using a $1\bar{1}$ spin-echo pulse sequence (Sklenář & Bax, 1987) to suppress the water resonance. For each RNA molecule and RNA peptide complex, a series of two-dimensional NMR spectra were acquired at one or more temperatures. For obtaining information on the nonexchangeable resonances observed in samples in D_2O, these included NOESY (Kumar *et al.*, 1980) spectra at several mixing times, P.COSY (Marion & Bax, 1988) spectra, and HOHAHA (Bax & Davis, 1985) spectra for each of the temperatures studied. In most cases, spectra were obtained at 50, 40, and 30 °C. The exchangeable proton resonances were monitored by obtaining NOESY spectra of the sample in H_2O by replacing the read pulse with a $1\bar{1}$ spin-echo pulse sequence. These were obtained at 1–10 °C, since above that temperature the exchange of most of the imino protons with H_2O becomes too fast to see NOE cross-peaks. Quadrature detection in two-dimensional experiments was obtained by the method of States *et al.* (1982). Data were transferred to a Silicon Graphics 4D/25 and processed with FTNMR/FELIX (Hare Research). NOESY spectra in H_2O were baseline flattened with a second-order polynomial in t_2, and residual water was subtracted using a time–domain convolution routine (Marion *et al.*, 1989). Detailed descriptions of other acquisition and processing parameters are given in the figure captions.

RESULTS

Imino Proton Spectra of RBE3 and Derivatives. The sequences and putative folded structures of RBE3, RBE3-A, and RBE3AA are shown in Figure 1, along with the wild-type sequence. One-dimensional spectra of the imino proton

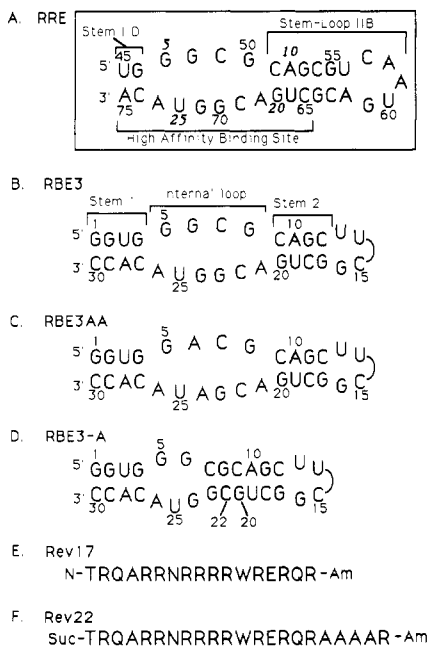

FIGURE 1: Sequence and proposed folding of (A) a portion of domain II of the RRE containing the core binding element defined by Bartel *et al.* (1991) and stem–loop IIB. The plain numbers are RRE numbering derived from Malim & Cullen (1991), and the italicized numbers are RBE3 numbering [figure modified from Bartel *et al.* (1991)]. (B) RBE3. The regions referred to in the text as stem 1, internal loop, and stem 2 as well as the numbering system used in the NMR study are indicated. (C) RBE3AA. G6 and G24 of RBE3 are replaced by A6 and A24. (D) RBE3-A. The same as RBE3 but with a deletion of A21. The numbering system of RBE3 is maintained. (E) Amino acid sequence of Rev17, which contains residues 34–50 of Rev and is amidated at the C terminus (Tan *et al.*, 1993). (F) Amino acid sequence of Rev22 (Tan *et al.*, 1993), which contains Rev_{34-50} plus four alanines and an arginine at the C terminus. Rev22 is succinylated at the N terminus and amidated at the C terminus.

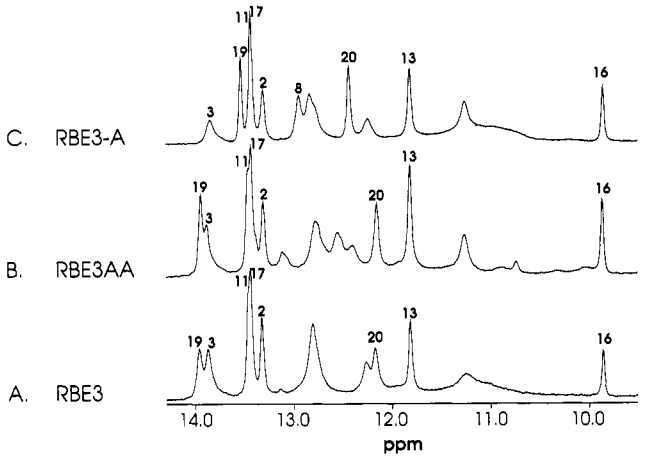

FIGURE 2: One-dimensional imino proton spectra at 1 °C of (A) REB3, (B) RBE3AA, and (C) RBE3-A. Samples were 2 mM RBE3 and RBE3-A or 3 mM RBE3AA in 10 mM phosphate, pH 6.5 (RBE3) or pH 5.9 (RBE3AA and RBE3-A), 100 mM NaCl, and 90% H_2O/10% D_2O. The spectra were acquired with 4096 complex points, 128 scans, and a spectral width of 10 000 Hz and apodized with a 70°-shifted sine-bell function.

resonances of RBE3 and the two derivatives are shown in Figure 2. The appearance of relatively sharp imino proton resonances in the chemical shift range normally associated with hydrogen-bonded bases indicates that all three molecules form specific hydrogen-bonded structures. The assignments of the imino proton resonances indicated on the figure were obtained from analysis of NOESY spectra of the samples in H_2O. The imino region of a NOESY spectrum of REB3 in

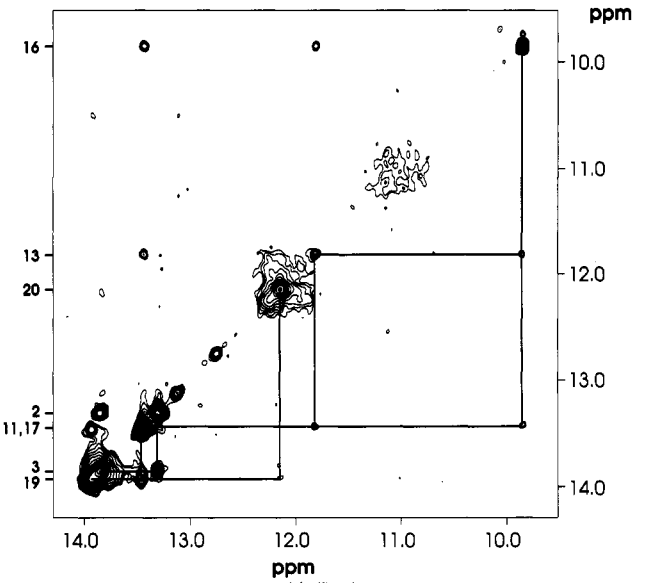

FIGURE 3: Portion of a contour plot of a NOESY spectrum of RBE3 in H_2O at 1 °C and τ_m = 150 ms, showing the imino proton region. Assignments of the imino protons are shown on the side of the spectrum. The sample was 2 mM RBE3 in 10 mM phosphate, pH 5.9, and 100 mM NaCl in 90% H_2O/10% D_2O. The spectrum was acquired with 1024 and 311 complex points in t_2 and t_1, respectively, 64 scans per t_1 increment, and a spectral width of 10 000 Hz in both dimensions and apodized with a 60°- and 70°-shifted squared sine bell in t_2 and t_1, respectively, and zero filled to 2048 points in both dimensions.

H_2O is shown in Figure 3. The strong imino–imino NOE between U13 and G16 provided evidence for formation of the expected UUCG tetraloop with a U·G base pair. These iminos resonate at chemical shifts almost identical to those reported for the U·G base pair in the UUCG tetraloop of GGACUUCGGUCC (Varani *et al.*, 1991) and provided confirmation of the sequential imino assignments at that end of the molecule. For RBE3 and RBE3AA, sequential imino connectivities are observed from base pair G2·C29 to U3·A28 and from C9·G20 through U13·G16. In RBE3-A, the latter sequential connectivities are extended one base pair through G8·C22. Additional imino proton resonance intensity in the chemical shift range of base-paired iminos in all three spectra could not be assigned due to more rapid exchange of these (broader) resonances with H_2O. The imino resonances must arise from base pairs in the internal loop or from base pairs G1·C30 or G4·C27.

NOESY Spectra and Assignments of Nonexchangeable Proton Resonances of RBE3. Sequential assignments of the base and H1′ resonances were obtained by analysis of NOESY, COSY, and HOHAHA spectra of the RNA molecules in D_2O using standard methods for nucleic acids [reviewed in Feigon *et al.* (1992), Varani and Tinoco (1991), and Wüthrich (1986)]. The base–H1′ region of the NOESY spectrum of RBE3 at 50 °C is shown in Figure 4A, and the identical region of the HOHAHA spectrum is shown in Figure 5. At this temperature, most of the NOESY cross-peaks are fairly well resolved. The chemical shifts of resonances from the C(UUCG)G hairpin loop portion of the molecule are nearly identical to those reported by Varani *et al.* (1991). Ambiguities in assignments due to spectral overlap were for the most part resolved by comparison of spectra obtained at several temperatures.

The A28H2 and A10H2 were initially assigned from the NOESY spectra in H_2O on the basis of cross-peaks from the imino proton resonances of U3 and U19, respectively. These

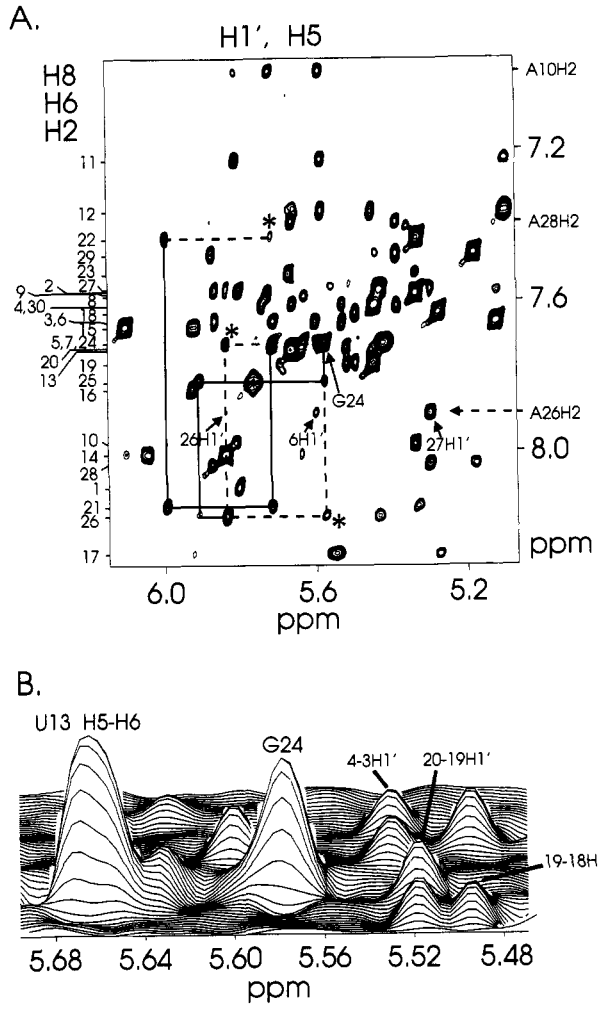

FIGURE 4: (A) Portion of a contour plot of a NOESY spectrum of RBE3 in D_2O at 50 °C and τ_m = 300 ms, showing the region containing the aromatic–H1′,H5 cross-peaks. Assignments of the H8 and H6 resonances are indicated on the side of the spectrum. Sequential connectivities from G24-U25-A26 and from G20-A21-C22 are indicated by solid lines. Nonsequential cross-peaks between G24 and A26 and between C22 and G20 are indicated by dashed lines (see Figure 6A). Cross-peaks between A26H2 and H1′ resonances are labeled. (B) Stacked plot of a part of the spectrum shown in (A). The intranucleotide G24H8–H1′ and U13H5–H6 and internucleotide G4H8–U3H1′, G20H8–U19H1′, and U19H6–C18H1′ NOE cross-peaks are labeled; unlabeled cross-peaks are intranucleotide base–H1′ NOEs. The sample was 2 mM in concentration in 10 mM phosphate, pH 5.9, and 100 mM NaCl in D_2O. The spectrum was acquired with 1024 and 317 complex points in t_2 and t_1, respectively, 32 scans per t_1 increment, and a spectral width of 4000 Hz in both dimensions and apodized with a 60°-shifted squared sine bell in t_2 and t_1 and zero filled to 2048 points in both dimensions.

assignments were used in confirming the sequential assignments, since the AH2s in RNA show cross-peaks to the 3′ neighboring H1′ and to the 5′ neighboring H1′ on the opposite strand (Varani *et al.*, 1989). The assignments of all four AH2 resonances were confirmed by their chemical shifts in a ^1H–^{15}N HSQC (Bodenhausen & Ruben, 1980) spectrum of a ^{15}N-labeled sample of RBE3. The ^1H–^{15}N HSQC spectrum provides unambiguous identification of AH2, CH5, CH6, UH5, UH6, and purine H8 resonances (Sklenář *et al.*, 1994).

The base–H1′ assignments were confirmed by analogous base–H2′ sequential connectivities. Due to the small H1′–H2′ coupling constants for many of the riboses in RBE3, only about half the possible H1′–H2′ cross-peaks were observed in COSY and HOHAHA spectra. Therefore, the H1′–H2′

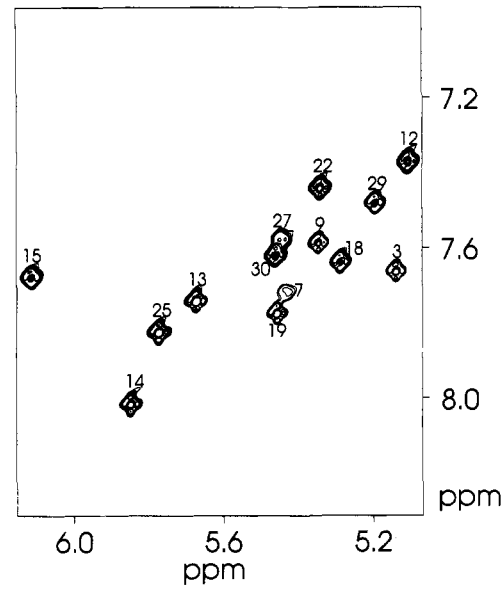

FIGURE 5: Portion of a HOHAHA spectrum of RBE3 in D_2O at 50 °C and τ_m = 100 ms, showing the pyrimidine H5–H6 cross-peaks. Assignments are indicated. The sample was 2 mM in concentration in 10 mM phosphate, pH 5.9, and 100 mM NaCl in D_2O. The spectrum was acquired with 2048 and 358 complex points in t_2 and t_1, respectively, 32 scans per t_1 increment, and a spectral width of 4000 Hz in both dimensions and apodized with a 60°-shifted squared sine bell in t_2 and t_1 and zero filled to 2048 points in both dimensions.

Table 1: Chemical Shifts (ppm) of Proton Resonances, Relative to DSS, for RBE3 at 50 °C in 100 mM NaCl and 10 mM Sodium Phosphate, pH 5.9

	H6/H8	H2/H5	H1′	H2′	H3′	H4′	imino[a]
5′ G1	8.10		5.80	4.90	4.69		
G2	7.57		5.87	4.56		4.50	13.33
U3	7.66	5.12	5.53	4.54			13.87
G4	7.61		5.66				
G5	7.71		5.71	4.63	4.39		
G6	7.76		5.60	4.51			
C7	7.71	5.42	5.63	4.51			
G8	7.59		5.73	4.50			
C9	7.58	5.34	5.34	4.40			
A10	7.98	6.99	5.81	4.52			
G11	7.23		5.58	4.35			13.45
C12	7.36	5.10	5.45	4.42	4.19	4.36	
U13	7.73	5.67	5.64	3.77	4.49	4.34	11.82
U14	8.01	5.84	6.04	4.63	4.01	4.44	
C15	7.67	6.10	5.92	4.06	4.47	3.77	
G16	7.84		5.93	4.80	5.55	4.37	9.86
G17	8.27		4.48	4.38			13.44
C18	7.63	5.27	5.50	4.44	4.36		
U19	7.77	5.45	5.52	4.41	4.51		13.96
G20	7.72		5.72	4.26			12.17
A21	8.15	7.98	6.00	4.64	4.68	4.48	
C22	7.44	5.33	5.33	4.19	4.31	4.36	
G23	7.53		5.67	4.36			
G24	7.72		5.58	4.66	4.42		
U25	7.82	5.76	5.91	4.38	4.65	4.51	
A26	8.17	7.90	5.84	4.70	4.53		
C27	7.57	5.43	5.30	4.28			
A28	8.03	7.39	5.87	4.47			
C29	7.48	5.18	5.39	4.06	4.48		
C30	7.61	5.44	5.74	3.97	4.06		

[a] Imino chemical shifts are at 1 °C, pH 6.5.

connectivities were obtained from a NOESY spectrum acquired with a mixing time of 100 ms. Only about half of the H3′ and a few H4′ were resolved in the COSY and HOHAHA spectra. The assignments of RBE3 are given in Table 1. Sequence-specific base and H1′ assignments were also obtained on a uniformly ^{15}N,^{13}C-labeled sample of RBE3 using two-dimensional HCNCH (Sklenář *et al.*, 1993b) as

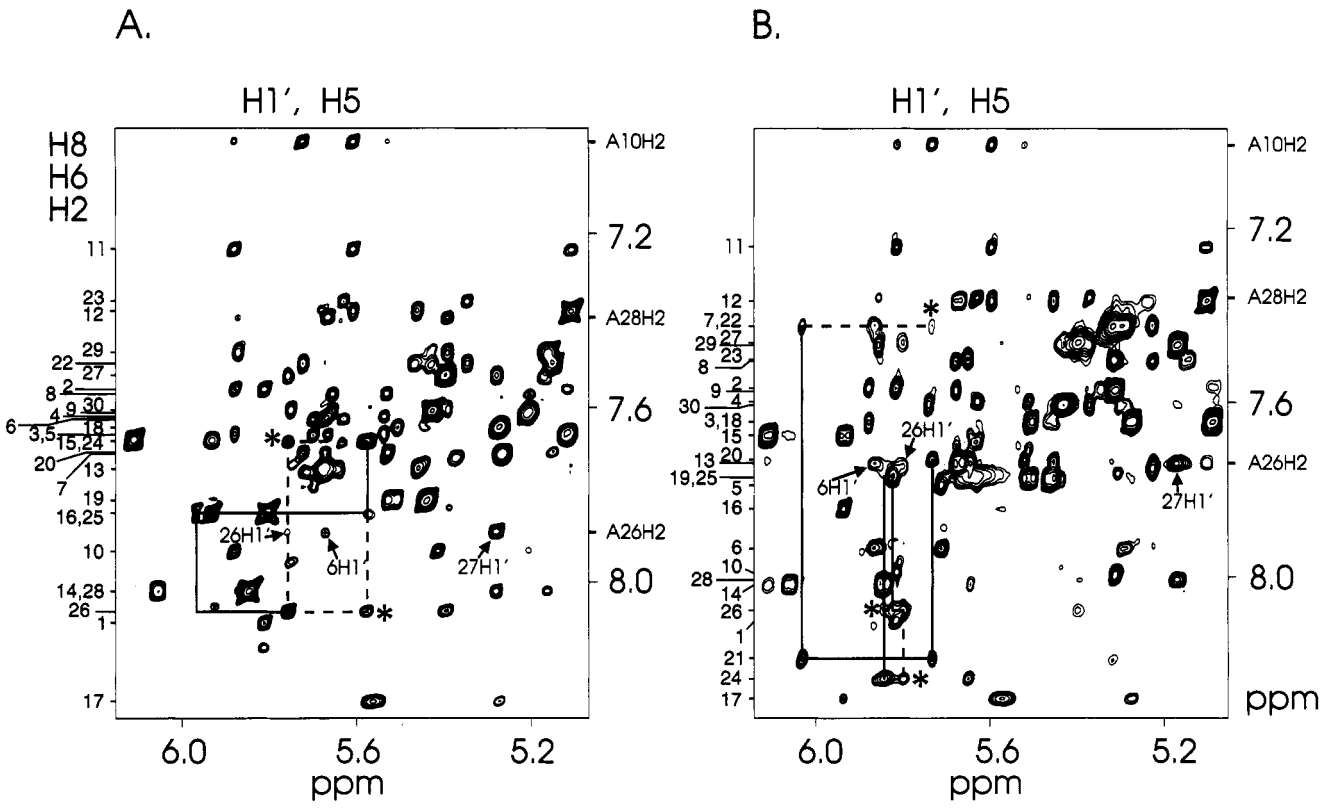

FIGURE 6: Portions of NOESY spectra of (A) RBE3-A and (B) RBE3AA in D_2O with τ_m = 300 ms, showing the region containing the aromatic–H1′,H5 cross-peaks. Assignments of the H8 and H6 resonances are indicated on the side of the spectrum. Sequential connectivities from (A) G24-U25-A26 and (B) A24-U25-A26 and G20-A21-C22 are indicated by solid lines. Nonsequential connectivities from (A) G24–A26 and (B) A24–A26 and C22–G20 are indicated by dashed lines. Cross-peaks between A26H2 and H1′ resonances are labeled. The sample in (A) was 2 mM RBE3-A in 10 mM phosphate, pH 5.9, and 100 mM NaCl at 50 °C. The spectrum was acquired with 512 and 365 complex points in t_2 and t_1, respectively, 32 scans per t_1 increment, and a spectral width of 4000 Hz in both dimensions and apodized with a 60°-shifted sine bell in t_2 and t_1 and zero filled to 2048 points in both dimensions. The sample in (B) was 3 mM RBE3AA in 10 mM phosphate, pH 5.9 and 100 mM NaCl at 45 °C. The spectrum was acquired with 1024 and 439 complex points in t_2 and t_1, respectively, 32 scans per t_1 increment, and a spectral width of 4000 Hz in both dimensions and apodized with a 60°-shifted sine bell in t_2 and a 70°-shifted squared sine bell in t_1 and zero filled to 2048 points in both dimensions.

well as two- and three-dimensional HCN (Sklenář *et al.*, 1993a) experiments.

NOE Connectivities in the "Purine-Rich Bubble" and near A21. Normal sequential base–H1′ connectivities are observed for most of the molecule. However, in the region of G24–A26 and C22–G20 there are some nonstandard A-RNA connectivities. The region G24–A26 and G5–G6 in the internal loop has been referred to as the purine-rich bubble (Heaphy *et al.*, 1991) and contains potential non-Watson–Crick base pairs. The intensity of the G24H8–H1′ cross-peak indicates that this nucleotide is in the *syn* conformation. A stacked plot of the NOESY spectrum of RBE3 showing the region containing the G24H8–H1′ cross-peak is shown in Figure 4B. The intensity of this cross-peak is comparable to that of U13H5–H6, indicating that G24H8 is close (~2.6 Å) to G24H1′ and therefore the nucleotide must be in the *syn* conformation. Although sequential connectivities are observed from G24 to U25 to A26, these are very weak relative to what is normally observed. In contrast, there are relatively strong NOE connectivities between G24 and A26, indicating that U25 is looped out of the helix and G24 and A26 are stacked on each other. In addition to the A26H8–G24H1′ cross-peak, there is a strong G24H8–A26H1′ cross-peak, which also indicates that G24 is *syn*. The observed NOEs for G24–A26 are indicated in Figure 4A and summarized schematically in Figure 10A. Although normal sequential base–H1′ connectivities are observed from G20-A21-C22, a nonsequential base–H1′ connectivity is also present between C22H6 and G20H1′. The relevant cross-peaks are indicated in Figure 4A.

NOESY Spectra of the Nonexchangeable Proton Resonances of RBE3-A and REB3AA. The NOESY spectra of RBE3-A and RBE3AA in D_2O are very similar to those of RBE3, and assignments were obtained in the same way. The base–H1′ regions of NOESY spectra of RBE3-A and RBE3AA are shown in Figure 6. The NOESY spectrum of RBE3-A is better resolved and has sharper lines than RBE3. The chemical shifts of the two molecules are essentially the same except for the resonances from C22 and G23, 3′ to the deleted A, and their respective pairing partners G8 and C7. NOE cross-peak intensities also indicate that G24 in RBE3-A is in the *syn* conformation.

The NOESY spectrum of RBE3AA (Figure 6B) has broader lines than those of RBE3, especially in the internal loop. Chemical shift differences from RBE3 are observed primarily for the resonances at and 3′ to the 6 and 24 positions where the A substitutions were made: G5, A6, C7, G8, A24, U25, and A26. In this molecule, it is not entirely clear whether A24 is *syn* or *anti*. The integrated intensity of the A24H8–H1′ cross-peak is not large enough to definitely indicate *syn*, but this cross-peak is also fairly broad. However, there is an A24H8–A26H1′ cross-peak, which should only be seen if A24 were *syn* (with U25 looped out). The U25H5 and H6 cross-peaks are also very broad. The line broadening for the resonances in the purine-rich bubble is consistent with some conformational exchange, especially for U25 and A24.

Temperature Dependence of NOESY Spectra of RBE3 and Derivatives. The appearance of the NOESY spectra of RBE3 and derivatives as a function of temperature indicates that

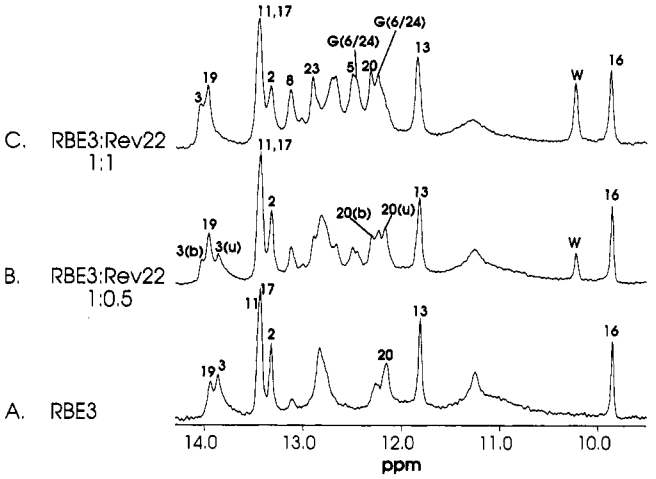

FIGURE 7: One-dimensional imino proton spectra at 1 °C of (A) RBE3, (B) 1:0.5 RBE3:Rev22, and (C) 1:1 RBE3:Rev22. RBE3 was 0.7 mM in concentration (A and B) or 1.5 mM (C) in 10 mM phosphate, pH 6, 100 mM NaCl, 0.1 mM EDTA, and 90% H_2O/10% D_2O. Spectra were acquired with 4096 complex points, 128 (A), 512 (B), or 256 (C) scans, and a spectral width of 10 000 Hz and apodized with a 70°-shifted sine bell.

there is some conformational averaging, especially in the internal loop region. NOESY spectra for RBE3 were obtained at 10, 20, 30, 40, and 50 °C. As the temperature is decreased below 40 °C, resonances and cross-peaks from the internal loop begin to broaden. The line broadening almost certainly arises from intermediate exchange (on the NMR time scale) between base-paired and open states and/or between alternative base-paired states [see Gilbert *et al.* (1989) for an example involving Hoogsteen A·T base pairs]. Significantly, the chemical shifts do not change appreciably from 10 to 50 °C (0.01–0.07 ppm changes). This indicates that the conformational exchange is either between two equally populated states or one predominant conformation with one or more minor conformations. The NOE data, however, are consistent with RBE3 forming one structure and therefore indicate that there is a predominant conformation. The narrower line widths at high temperatures are due to faster conformational exchange at these temperatures and/or increase in the major conformation.

RBE3-A has sharper lines and better resolved NOESY spectra than RBE3 at all temperatures studied, although line broadening in the internal loop still occurs below 40 °C. In contrast, the spectra of RBE3AA have broader lines than those of RBE3 at all temperatures studied. These results are consistent with the sequences of the RNA molecules. In RBE3-A, the only region of the molecule where there could be non-Watson–Crick or unpaired bases (besides the UUCG loop) is the purine-rich bubble, and therefore alternative conformations are most likely limited to this region. In RBE3AA, the substitution of A6 and A24 for G6 and G24 also introduces a potential new Watson–Crick A6·U25 base pair in addition to the proposed A6·A24 base pair. Conformational exchange between these alternative base pairs may account for the line broadening observed.

NMR Spectra of the RBE3–Rev Peptide Complexes. ^1H NMR spectra were obtained on complexes of RBE3 with Rev17 and Rev22 peptides. These peptides contain residues 34–50 of Rev (Rev17) and residues 34–50 plus four alanines and an arginine at the C-terminal end of the peptide (Rev22). The peptides were titrated into samples of RBE3, and binding was initially monitored by changes in the imino proton spectra (Figure 7). At less than stoichiometric amounts of peptide,

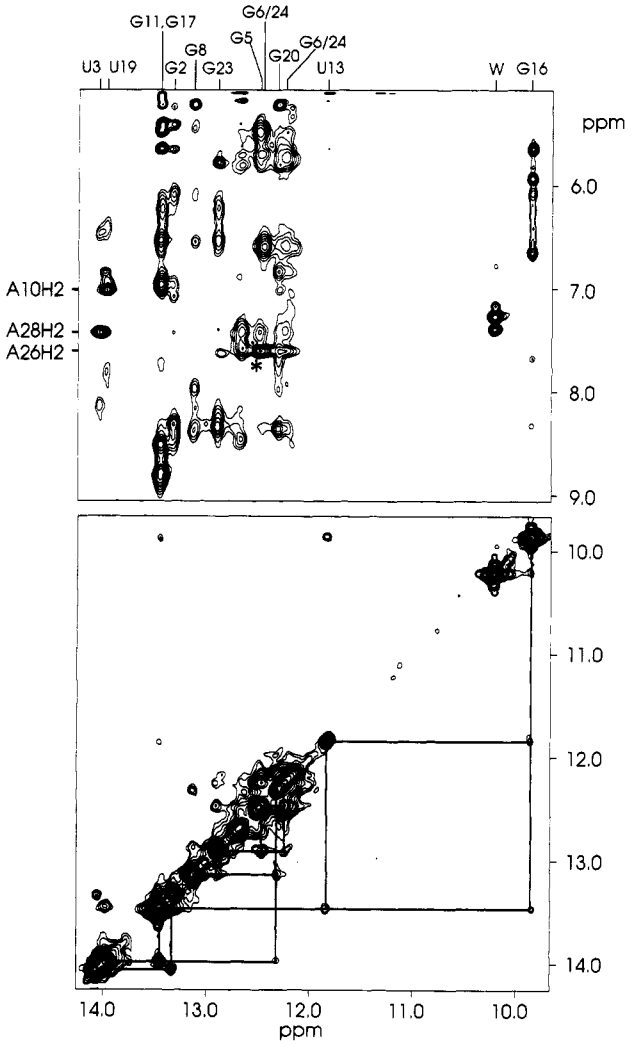

FIGURE 8: Portion of a NOESY spectrum of 1:1 RBE3:Rev22 at 1 °C with τ_m = 100 ms, showing the imino protons (lower region) and the imino–amino, aromatic, and H1′ region (upper region). Sequential imino–imino connectivities are indicated by solid lines. The asterisk indicates the G5 imino to A26H2 cross-peak. RBE3 and Rev22 were 1.5 mM in concentration; all other sample conditions are as in Figure 4. The spectrum was acquired with 1024 and 266 complex points in t_2 and t_1, respectively, 128 scans per t_1 increment, and a spectral width of 10 000 Hz in both dimensions and apodized with a 70°-shifted sine bell in t_2 and t_1 and zero filled to 2048 points in both dimensions.

two sets of resonances are observed corresponding to the free RBE3 and a 1:1 RBE3:Rev peptide complex. Some additional slowly exchanging imino resonances that gave rise to cross-peaks in NOESY spectra also appear.

In the 1:1 RBE3–Rev22 complex, the sequential imino–imino connectivities are extended four base pairs (relative to free RBE3) from C9·G20 to G8·C22 to C7·G23 to G6·G24 to G5·A26 (Figure 8). A strong G6–G24 imino–imino cross-peak confirms the presence of a G6·G24 base pair of the type shown in Figure 10C. The presence of a G5·A26 base pair is confirmed by a strong G5 imino to A26H2 cross-peak (Figure 8). Only the G1·C30 and G4·C27 iminos and the non-base-paired U25 and U14 iminos do not give rise to observable NOE cross-peaks in the RBE3–Rev22 complex.

Although the NOESY spectra of the exchangeable resonances in the complex have sharper lines than imino spectra of the free RNA, NOESY spectra of the complex in D_2O show significant line broadening of the nonexchangeable resonances from most of the internal loop. We initially studied

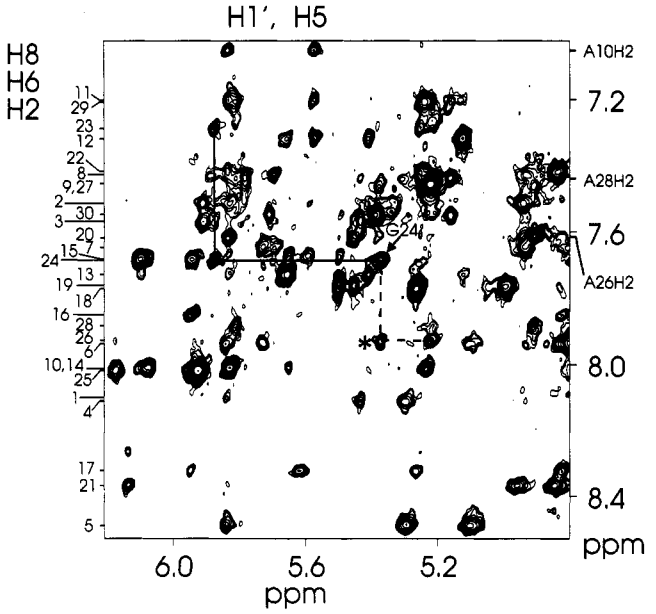

FIGURE 9: Portion of a NOESY spectrum of 1:1 RBE3:Rev22 in D_2O at 30 °C and τ_m = 350 ms, showing the region containing the RNA aromatic–H1′,H5 cross-peaks. Assignments of the H8 and H6 resonances are indicated on the side of the spectrum. Connectivities from G23–G24 are indicated with solid lines and from G24–A26 with dashed lines. Note that there is no cross-peak from G24H8 to A26H1′. RBE3 and Rev22 were 1 mM in concentration in 10 mM phosphate, pH 6, and 30 mM NaCl in D_2O. The spectrum was acquired with 1024 and 400 complex points in t_2 and t_1, respectively, 32 scans per t_1 increment, and a spectral width of 5000 Hz in both dimensions and apodized with a 60°-shifted sine bell in t_2 and t_1 and zero filled to 2048 points in both dimensions.

the complex under the same salt conditions used for the free RNA (10 mM phosphate, pH 6, and 100 mM NaCl). Under these conditions, much of the internal loop was not assignable due to line broadening. However, when the NaCl concentration was lowered to 30 mM, narrower line widths were observed, and we were able to obtain assignments of the RNA resonances of the internal loop. The chemical shifts of all resonances that were assignable under both salt conditions are virtually the same. This indicates that while the RNA–peptide complex has a smaller K_d at lower salt concentration, the structure of the complex is the same at both salt concentrations. Even under the low salt conditions many of the nonexchangeable cross-peaks are still very broad, indicating that there is probably exchange between bound and unbound forms. Figure 9 shows the base–H1′ region of a D_2O NOESY of the RBE3–Rev22 complex. G24 is in the *syn* conformation in the complex as well as in the free RNA. The integrated intensity of the G24H8–G24H1′ cross-peak indicates thatthe H8–H1′ distance is about 3 Å, which is longer than in the free RNA but within the range for the *syn* conformation. The G24H8–A26H1′ cross-peak seen in the free RNA is not present in the NOESY spectrum of the complex (see Figure 9). This may indicate that the RNA structure changes somewhat on Rev peptide binding. There are some large chemical shift differences between resonances of the Rev high-affinity binding site of the free and the bound RNA (see Table 2). Only preliminary assignments of the Rev peptide in the RBE3–Rev22 complex have been obtained. Observed peptide–RNA NOEs to G4, G5, and U25 proton resonances in the major groove indicate that the peptide binds specifically to the internal loop in the major groove as expected (Iwai *et al.*, 1992; Kjems *et al.*, 1992).

The imino proton spectrum of the RBE3–Rev17 complex looks similar to that of RBE3–Rev22. The major difference

Table 2: Chemical Shifts (ppm) of RNA Proton Resonances for RBE3 (Free) and the RBE3–Rev22 Complex (Bound) at 30 °C

	H6/H8			H2/H5			H1′		
	free[a]	bound[b]	Δ[c]	free	bound	Δ	free	bound	Δ
5′G1	8.12	8.1					5.80	5.82	
G2	7.55	7.51					5.89	5.91	
U3	7.67	7.57	–0.1	5.10	4.20	–0.9	5.51	5.43	
G4	7.61	8.12	0.51				5.67	5.30	–0.37
G5	7.72	8.49	0.77				5.74	5.84	0.1
G6	7.66	7.94	0.28				5.64	5.73	
C7	7.72	7.64		5.34	4.94	–0.4	5.60	5.69	
G8	7.55	7.43	–0.12				5.74	5.78	
C9	7.57	7.46	–0.11	5.33	5.22	–0.11	5.31	5.24	
A10	7.99	8.02		6.97	7.05		5.80	5.83	
G11	7.27	7.21					5.61	5.58	
C12	7.36	7.32		5.11	5.13		5.45	5.41	
U13	7.73	7.73		5.68	5.66		5.65	5.65	
U14	8.01	8.01		5.84	5.83		6.07	6.08	
C15	7.68	7.69		6.11	6.10		5.94	5.94	
G16	7.84	7.85					5.94	5.95	
G17	8.29	8.33							
C18	7.67	7.77	0.1	5.25	5.27		5.50	5.50	
U19	7.79	7.76		5.47	5.00	–0.47	5.52	5.45	
G20	7.73	7.62	–0.11				5.73	5.84	0.11
A21	8.18	8.37	0.19				6.01	6.14	0.13
C22	7.46	7.42		5.32	4.84	–0.48	5.32	5.25	
G23	7.54	7.29	–0.25				5.69	5.88	0.19
G24	7.73	7.69					5.60	5.37	–0.23
U25	7.86	8.02	0.16	5.78	5.93	0.15	5.94	6.17	0.23
A26	8.15	7.93	–0.23	7.87	7.62	–0.25	5.84	5.22	–0.62
C27	7.58	7.46	–0.12	5.38	5.23	–0.15	5.32	4.91	–0.41
A28	8.04	7.88	–0.16	7.34	7.44	0.1	5.87	5.81	
C29	7.49	7.21	–0.28	5.16	5.24		5.37	5.16	–0.21
C30	7.60	7.55		5.41	5.39		5.72	5.71	

[a] Sample is 10 mM phosphate, pH 5.9, 100 mM NaCl, and 2 mM RBE3. [b] Sample is 10 mM phosphate, pH 6.0, 30 mM NaCl, and 1 mM RBE3 + Rev22. [c] Chemical shift difference of >0.1 ppm are given.

is that the G5 imino is not seen. NOESY spectra of this complex in D_2O also show significant line broadening, and assignments through much of the internal loop could not be made at 10 mM phosphate, pH 6, and 100 mM NaCl. Together, these results indicate that Rev22 binds RBE3 only slightly better than Rev17.

DISCUSSION

The long-range goal of this work is to determine what structural elements are present in the high-affinity Rev binding site of the RRE, both when free and when bound by Rev. We therefore chose to study RBE3, an RNA molecule which contains the minimal wild-type high-affinity binding site, and two derivatives, REB3AA and RBE3-A. In their *in vitro* selection experiments for Rev binding to a uniformly mutated RRE domain II, Bartel *et al.* (1991) found a covariation of the highly conserved G48 and G71 with A's. Since G·G and A·A can form isosteric base pairs, they proposed that G48 and G71 form a *syn·anti* base pair as shown in Figure 10C, although they could not predict which base should be *syn*. Similar *syn·anti* homopurine pairing in ribosomal RNA has been proposed by Gutell and Woese (1990) on the basis of multiple transitions between G·G and A·A. RBE3AA, a derivative of RBE3 in which the G's analogous to G48 and G71 are replaced by A's, was studied to help test this idea. Heaphy *et al.* (1991) and Kjems *et al.* (1992) found that deletion of A68 of the RRE had only a small effect on Rev binding. The deletion of A21 (analogous to A68 of the RRE) from RBE3, yielding RBE3-A, extends stem 2 by two base pairs and thus provides a potentially more stable RNA structure.

Conformation of the RRE High-Affinity Rev Binding Site. The NMR spectra of RBE3, RBE3AA, and RBE3-A indicate

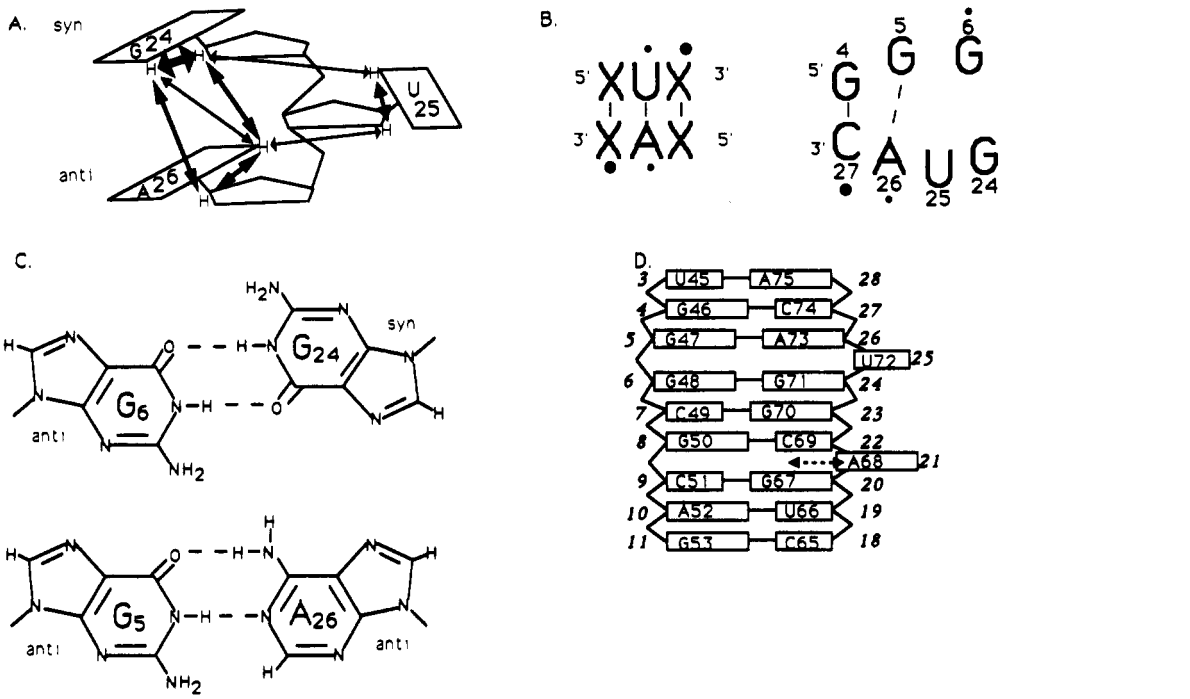

FIGURE 10: (A) Schematic illustrating the sequential and nonsequential base–H1′ NOE cross-peaks observed between and proposed stacking of G24, U25, and A26. The thickness of the lines corresponds to the relative intensities of the NOEs observed. Note that G24 is *syn*. (B) (Left) Pattern of NOE cross-peaks from AH2 to nearby H1′ protons which is normally observed in Watson–Crick base-paired RNA. (Right) NOE cross-peaks from A26H2 to nearby H1′ protons which are observed (see Figure 3A). (C) Base-paired structures of G6·G24 and G5·A26 in RBE3 consistent with the NMR data. (D) Schematic illustration of base pairing and stacking of the RRE high-affinity Rev binding site in the presence of Rev 22 consistent with the NMR data. Italicized numbers are RBE3 numbering. In the absence of peptide, the predominant conformation is the same, except that A68 appears to be stacked in the helix at least part of the time (dashed arrow).

that all three molecules fold into the expected stem–internal loop–stem–hairpin loop structure. This basic folded structure is very stable, with a T_m above 60 °C. The two four-base stems and the UUCG tetraloop are clearly established by the NMR data. The interesting question is, what is the structure of the internal loop? Although it is not possible to assign imino resonances in the internal loop, it cannot be concluded from this that the internal loop is unstructured. Slowly exchanging imino resonances are also not observed for the terminal G·C base pair. This is commonly the case in nucleic acids and is attributed to faster exchange of the iminos at the ends of a helix (fraying), rather than absence of base pairs. The additional unassigned imino resonance intensity is consistent with some hydrogen bonding in the internal loop. The broader line widths and the fact that these resonances show no NOESY cross-peaks are consistent with faster exchange with water protons and/or conformational averaging, i.e., alternative base pairs or equilibrium between open and closed states.

Evidence for conformational averaging in the internal loops of these molecules is seen in the nonexchangeable spectra. However, as discussed earlier, the NMR data indicate that the internal loops of RBE3 and RBE3-A have a predominant conformation. The major conformation of RBE3 is illustrated schematically in Figure 10. G24 in both RBE3 and RBE3-A is in the *syn* conformation. The case of RBE3AA is less clear, although the data are consistent with A24 being *syn* at least some of the time. This, combined with the prediction by Bartel *et al.* (1991) that G48 and G71 of the RRE form an *anti·syn* base pair, argues very strongly that a $G6_{anti}$·$G24_{syn}$ base pair (Figure 10C) forms in RBE3 and RBE3-A and that an isosteric $A6_{anti}$·$A24_{syn}$ base pair forms in RBE3AA at least part of the time. U25 is looped out of the helix with A26 stacked on G24/A24 in the major conformation of all three molecules. The base stacking and important NOEs are illustrated schematically in Figure 10A. The looping out of U25 is consistent with the nucleotide analogue studies of Iwai *et al.* (1992), who showed that the identity of the base in position 72 of the RRE was unimportant for Rev binding and suggested that U72 serves as a spacer for G48·G71 and G47·A73 base pairs on either side.

The NOESY spectra also provide evidence for a G5·A26 base pair. A26H2 has NOESY cross-peaks to G6H1′ (A6H1′ in RBE3AA), A26H1′, and C27H1′ in all three molecules (Figure 4A and Figure 6). This pattern of cross-peaks would be expected for A26 stacked in the helix and base paired to G5 (Figure 10B). The fact that the A26H2–G6H1′ cross-peak is weak and that there is no cross-peak to G5H1′ suggests that this postulated base pair is wider than a Watson–Crick base pair and/or that G5 and A26 are in equilibrium between being base paired and being looped out. Of the several types of G·A base pairs previously observed in DNA oligonucleotides, our data are most consistent with the G_{anti}·A_{anti} form shown in Figure 10C (Kan *et al.*, 1983; Patel *et al.*, 1984; Privé *et al.*, 1987). Possible pairings in which one base is *syn* are eliminated because both G5 and A26 are *anti*. Sequential NOE connectivities indicate that both G5 and A26 stack normally in their respective strands, while the "sheared" *anti·anti* conformation gives cross-strand stacking (Chou *et al.*, 1992).

NOESY spectra of RBE3 and RBE3AA in D_2O show a cross-peak from C22H6 to G20H1′. This, together with the low-field chemical shifts of A21H8 and H2, would seem to indicate that A21 is looped out of the helix. However, normal sequential connectivities from G20 to A21 to C22 suggest that A21 is stacked into the helix (Figure 4A and Figure 6). These data suggest that in the free RNA A21 is sometimes stacked into the helix and sometimes looped out. The structural features of the conformation of the RRE high-

affinity Rev binding site are shown schematically in Figure 10D.

Conformation of RBE3 When Bound to Rev Peptide. When RBE3 is bound to Rev peptide, new slowly exchanging imino proton resonances appear. The additional imino resonance intensity observed upon binding of the Rev peptides to the RNA could be the result of stabilization of the base pairs in the internal loop upon peptide binding and/or decreased solvent accessibility as a consequence of peptide binding. Addition of Mg^{2+} to the free RBE3 did not result in any changes in the imino proton spectra (not shown), but we do not know if this is the case with other polycations. Assignment of the imino resonances gives direct evidence for hydrogen-bonded iminos in non-Watson–Crick base pairs in the internal loop region of RBE3. In the RBE3–Rev22 complex, imino–imino connectivities can be followed from G16·U13 to G5·A26, giving direct evidence for G8·C22 and C77·G23 base pairs, as well as for G6·G24 and G5·A26 base pairs. The strong G6–G24 imino–imino cross-peak shows that G6 and G24 are hydrogen bonded as shown in Figure 10C, since this is the only type of G·G base pair that utilizes the iminos of both G's for H-bonding (Saenger, 1984). The strong G5 imino to A26H2 cross-peak indicates that the G5·A26 base pair is in the extended *anti·anti* conformation, since this is the only type of G·A base pair in which the H-bonded G imino is close to the AH2 (Saenger, 1984). This is also consistent with the nucleotide analogue studies of Iwai *et al.* (1992), whose results showed that G47 and A73 of the RRE formed either a G_{anti}·A_{anti} or a G_{anti}·A_{syn} base pair when bound by Rev. "Sequential" imino–imino cross-peaks from C9·G20 imino to G8·C22 imino and from G(6 or 24) imino to G5·A26 imino indicate respectively that A21 and U25 are looped out of the helix in the RBE3–Rev22 complex.

Large chemical shift changes which occur primarily in the resonances from nucleotides in the core binding element of RBE3 indicate specific binding of Rev22 to RBE3. However, the broadening of the nonexchangeable resonances in the internal loop of RBE3 indicates that the exchange between bound and unbound forms of the RNA is intermediate on the NMR time scale. Thus, under the NMR conditions used in these studies, the K_d of the RBE3–Rev22 complex is greater than the reported subnanomolar K_d of Rev22 to an almost identical RNA molecule (Tan *et al.*, 1993).

Conclusions. The internal loop of RBE3 is in conformational exchange between two or more conformations, possibly involving different base-pairing schemes. There is a major conformation which contains several distinct structural features. In the purine-rich bubble, G6 and G24 form an *anti·syn* base pair and G5 and A26 are stacked in position to form an *anti·anti* base pair. U25 is looped out of the helix. These structural features are confirmed by the analogous results with RBE3AA and RBE3-A. When RBE3 is bound by Rev22, these features of the internal loop remain and appear to be stabilized. Imino proton resonances corresponding to G6·G24 and G5·A26 base pairs are observed. In the free RNA, A21 is conformationally flexible and appears to be in equilibrium between being stacked in and looped out of the helix. However, in the RBE3–Rev22 complex, A21 is looped out.

This model system of RBE3 and Rev peptides has provided insight into the structure of the RRE high-affinity Rev binding site, both free and when complexed with Rev. It is interesting to compare these results to the structure of the HIV-1 TAR RNA Tat binding site (Puglisi *et al.*, 1992, 1993). On the basis of the NMR data, Puglisi *et al.* concluded that the structure of the Tat binding region of the free TAR RNA is not well-defined, but when bound by argininamide (as a model for Tat protein) the RNA undergoes a major conformational change and becomes highly structured. In contrast, the data presented here suggest a model in which the predominant structure of the high-affinity Rev binding site of the free RRE contains major structural features in common with the RNA when bound by Rev protein. Thus, we propose that Rev protein recognizes and binds to specific structural elements of the RRE.

REFERENCES

Bartel, D. P., Zapp, M. L., Green, M. R., & Szostak, J. W. (1991) *Cell 67*, 529–536.

Bax, A., & Davis, D. G. (1985) *J. Magn. Reson. 65*, 355–360.

Bodenhausen, G., & Ruben, D. (1980) *Chem. Phys. Lett. 69*, 185–189.

Chang, D. D., & Sharp, P. A. (1989) *Cell 59*, 789–795.

Chou, S.-H., Cheng, J.-W., & Reid, B. R. (1992) *J. Mol. Biol. 228*, 138–155.

Cochrane, A. W., Chen, C.-H., & Rosen, C. A. (1990) *Proc. Natl. Acad. Sci. U.S.A. 87*, 1198–1202.

Cook, K. S., Fisk, G. J., Hauber, J., Usman, N., Daly, T. J., & Rusche, J. R. (1991) *Nucleic Acids Res. 19*, 1577–1583.

D'Agostino, D. M., Felber, B. K., Harrison, J. E., & Pavlakis, G. N. (1992) *Mol. Cell. Biol. 12*, 1375–1386.

Daly, T. J., Cook, K. S., Gray, G. S., Maione, T. E., & Rusche, J. R. (1989) *Nature 342*, 816–819.

Dayton, E. T., Koning, D. A. M., Powell, D. M., Shapiro, B. A., Butini, L., Maizel, J. V., & Dayton, A. I. (1992) *J. Virol. 66*, 1139–1151.

Emerman, M., Vazeux, R., & Peden, K. (1989) *Cell 57*, 1155–1165.

Feigon, J., Sklenář, V., Wang, E., Gilbert, D. E., Macaya, R. F., & Schultze, P. (1992) in *Methods in Enzymology* (Lilley, D. M. J., & Dahlberg, J. E., Eds.) pp 235–253, Academic Press, Inc., San Diego, CA.

Felber, B. K., Hadzopoulou-Cladaras, M., Cladaras, C., Copeland, T., & Pavlakis, G. N. (1989) *Proc. Natl. Acad. Sci. U.S.A. 86*, 1495–1499.

Gilbert, D. E., Van Der Marel, G. A., Van Boom, J., & Feigon, J. (1989) *Proc. Natl. Acad. Sci. U.S.A. 86*, 3006–3010.

Gutell, R. R., & Woese, C. R. (1990) *Proc. Natl. Acad. Sci. U.S.A. 87*, 663–667.

Hammarskjöld, M.-L., Heimer, J., Hammarskjöld, B., Sangwan, I., Albert, L., & Rekosh, D. (1989) *J. Virol. 63*, 1959–1966.

Heaphy, S., Dingwall, C., Ernberg, I., Gait, M. J., Green, S. M., Karn, J., Lowe, A. D., Singh, M., & Skinner, M. A. (1990) *Cell 60*, 685–693.

Heaphy, S., Finch, J. T., Gait, M. J., Karn, J., & Singh, M. (1991) *Proc. Natl. Acad. Sci. U.S.A. 88*, 7366–7370.

Holland, S. M., Ahmad, N., Maitra, R. K., Wingfield, P., & Venkatesan, S. (1990) *J. Virol. 64*, 5966–5975.

Huang, X., Hope, T. J., Bond, B. L., McDonald, D., Grahl, K., & Parslow, T. G. (1991) *J. Virol. 65*, 2131–2134.

Iwai, S., Pritchard, C., Mann, D. M., Karn, J., & Gait, M. J. (1992) *Nucleic Acids Res. 20*, 6465–6472.

Kan, L.-S., Chandrasegaran, S., Pulford, S. M., & Miller, P. S. (1983) *Proc. Natl. Acad. Sci. U.S.A. 80*, 4263–4265.

Kjems, J., & Sharp, P. A. (1993) *J. Virol. 67*, 4769–4776.

Kjems, J., Brown, M., Chang, D. D., & Sharp, P. A. (1991a) *Proc. Natl. Acad. Sci. U.S.A. 88*, 683–687.

Kjems, J., Frankel, A. D., & Sharp, P. A. (1991b) *Cell 67*, 169–178.

Kjems, J., Calnan, B. J., Frankel, A. D., & Sharp, P. A. (1992) *EMBO J. 11*, 1119–1129.

Kumar, A., Ernst, R. R., & Wüthrich, K. (1980) *Biochem. Biophys. Res. Commun. 95*, 1–6.

Lawrence, J. B., Cochrane, A. W., Johnson, C. V., Perkins, A., & Rosen, C. R. (1991) *New Biol. 3*, 1220–1232.

Lu, X., Heimer, J., Rekosh, D., & Hammarskjöld, M.-L. (1990) *Proc. Natl. Acad. Sci. U.S.A. 87*, 7598–7602.
Malim, M. H., & Cullen, B. R. (1991) *Cell 65*, 241–248.
Malim, M. H., Hauber, J., Le, S.-Y., Maizel, J. V., & Cullen B. R. (1989) *Nature 338*, 254–257.
Malim, M. H., Tiley, L. S., McCarn, D. F., Rusche, J. R., Hauber, J., & Cullen, B. R. (1990) *Cell 60*, 675–683.
Marion, D., & Bax, A. (1988) *J. Magn. Reson. 80*, 528–533.
Marion, D., Ikura, M., & Bax, A. (1989) *J. Magn. Reson. 84*, 425–430.
Milligan, J. F., Groebe, D. R., Witherell, G. W., & Uhlenbeck, O. C. (1987) *Nucleic Acids Res. 15*, 8783–8793.
Patel, D. J., Kozlowski, S. A., Ikuta, S., & Itakura, K. (1984) *Biochemistry 23*, 3207–3217.
Privé, G. G., Heinemann, U., Chandrasegaran, S., Kan, L.-S., Kopka, M. L., & Dickerson, R. E. (1987) *Science 238*, 498–504.
Puglisi, J. D., Tan, R., Calnan, B. J., Frankel, A. D., & Williamson, J. R. (1992) *Science 257*, 76–80.
Puglisi, J. D., Chen, L., Frankel, A. D., & Williamson, J. R. (1993) *Proc. Natl. Acad. Sci. U.S.A. 90*, 3680–3684.
Rosen, C. A. (1991) *Trends Genet. 7*, 9–14.
Rosen, C. A., Terwilliger, E., Dayton, A., Sodroski, J. G., & Haseltine, W. A. (1988) *Proc. Natl. Acad. Sci. U.S.A. 85*, 2071–2075.
Saenger, W. (1984) *Principles of Nucleic Acid Structure*, Springer-Verlag, New York.
Sklenář, V., & Bax, A. (1987) *J. Magn. Reson. 75*, 378–383.
Sklenář, V., Peterson, R. D., Rejante, M. R., & Feigon, J. (1993a) *J. Biomol. NMR 3*, 721–727.
Sklenář, V., Peterson, R. D., Rejante, M. R., Wang, E., & Feigon, J. (1993b) *J. Am. Chem. Soc. 115*, 12181–12182.
Sklenář, V., Peterson, R. D., Rejante, M. R., & Feigon, J. (1994) *J. Biomol. NMR 4*, 117–122.
States, O. J., Haberkorn, R. A., & Ruben, D. J. (1982) *J. Magn. Reson. 48*, 286–292.
Steffy, K., & Wong-Staal, F. (1991) *Microbiol. Rev. 55*, 193–205.
Tan, R., Chen, L., Buettner, J. A., Hudson, D., & Frankel, A. D. (1993) *Cell 73*, 1031–1040.
Tiley, L. S., Malim, M. H., Tewary, H. K., Stockley, P. G., & Cullen, B. R. (1992) *Proc. Natl. Acad. Sci. U.S.A.* 758–762.
Tuerk, C., MacDougal, S., Hertz, G. Z., & Gold, L. (1993) in *The Polymerase Chain Reaction* (Ferre, R., Mullis, K., Gibbs, R., & Ross, A., Eds.) Birkhauser, Springer-Verlag, New York (in press).
Varani, G., & Tinoco, I., Jr. (1991) *Q. Rev. Biophys. 24*, 479–532.
Varani, G., Wimberly, B., & Tinoco, I., Jr. (1989) *Biochemistry 28*, 7760–7772.
Varani, G., Cheong, C., & Tinoco, I., Jr. (1991) *Biochemistry 30*, 3280–3289.
Wüthrich, K. (1986) *NMR of Proteins and Nucleic Acids*, John Wiley & Sons, New York, NY.
Wyatt, J. R., Chastain, M., & Puglisi, J. D. (1991) *BioTechniques 11*, 764–769.
Zapp, M. L., & Green, M. R. (1989) *Nature 342*, 714–716.
Zawadzki, V., & Gross, H. J. (1991) *Nucleic Acids Res. 19*, 1948.